Proc. Natl. Acad. Sci. USA
Vol. 85, pp. 2146–2150, April 1988
Biophysics

High-sensitivity neutron diffraction of membranes: Location of the Schiff base end of the chromophore of bacteriorhodopsin

(purple membrane/*Halobacterium halobium*/retinal)

M. P. HEYN, J. WESTERHAUSEN, I. WALLAT, AND F. SEIFF*

Biophysics Group, Department of Physics, Freie Universität Berlin, Arnimallee 14, D-1000 Berlin 33, Federal Republic of Germany

Communicated by Walther Stoeckenius, November 6, 1987

ABSTRACT **Three important events in the functional cycle of bacteriorhodopsin occur at the chromophore: the primary absorption of light, the isomerization from the all-trans to the 13-cis form, and the deprotonation and reprotonation of its Schiff base. The protonated Schiff base linkage of the chromophore with lysine-216 plays an essential role in the color regulation of the pigment and is most likely directly involved in the charge translocation of this light-driven proton pump. Although much is known about the structure of the protein, the position of this key functional group has not yet been determined. We have synthesized a retinal in which the five protons closest to the Schiff base are replaced by deuterons. The labeled retinal was spontaneously incorporated into bacteriorhodopsin by using a mutant of *Halobacterium halobium* that is deficient in the synthesis of retinal. The position of the labeled Schiff base end of the chromophore was determined in the two-dimensional projected density of dark-adapted bacteriorhodopsin by neutron diffraction. The result fits very well with our previous work using retinals that were selectively deuterated in the middle of the polyene chain or in the cyclohexene ring. A coherent structure emerges with the three labeled positions on one line, separated by distances that are in good agreement with the tilt angle of the polyene chain (about 20°). The chromophore is located in the interior of the protein with the nitrogen of the Schiff base between helices 2 and 6 and with its ring in the vicinity of helix 4. Our results show that it is possible to locate a small group containing as few as five deuterons in a membrane protein of molecular weight 27,000.**

The chromophore of bacteriorhodopsin consists of retinal that is attached via a protonated Schiff base to lysine-216, a residue in the membrane-spanning helix G (1). Because of its essential role in the function of bacteriorhodopsin, we have investigated the position of this part of the chromophore in the plane of the membrane. Within the purple membrane, bacteriorhodopsin is arranged in a two-dimensional hexagonal lattice allowing the use of diffraction methods (2–9). In this way a structural model was obtained at a resolution of 3.5 Å in-plane (9). Due to its low electron density, however, the chromophore could not be resolved. In the light-adapted state of bacteriorhodopsin, the retinal is in the extended all-trans form having a length of approximately 15 Å (see Fig. 1). Since the angle between the polyene chain and the plane of the membrane is only about 20° (10), the projection of the chromophore onto this plane is elongated as well. Neutron diffraction provides an elegant method to obtain detailed structural information on the in-plane location and orientation of the various parts of the chromophore by using partially deuterated retinals (11, 12). The method takes advantage of the very large difference in neutron scattering length between hydrogen (protium, ^1H) and deuterium (^2H). Replacing ^1H by ^2H has the great advantage that it does not affect the electronic structure, as would be the case with a heavy atom. In order to localize the end of the polyene chain near the Schiff base, a retinal was synthesized with five deuterons as close as possible to the terminal carbon C-15. This retinal, [14,15,20,20,20-$^2H_5$]retinal ([$^2H_5$]retinal), has three deuterons in the C-13 methyl group and one deuteron each at C-14 and C-15 (Fig. 1). Bacteriorhodopsin samples containing [$^2H_5$]retinal and unlabeled retinal were prepared as described (11, 12), by adding them to the growth medium of the retinal-minus mutant JW5, which cannot synthesize retinal. The added retinals are incorporated spontaneously and form the normal pigment. This gentle biosynthetic procedure does not require any chemical manipulation of the purple membranes and leads to a hexagonal lattice of excellent quality. The position of the labeled group was determined from the difference in neutron diffraction intensities between a sample regenerated with [$^2H_5$]retinal and a sample regenerated in the same way with undeuterated retinal.

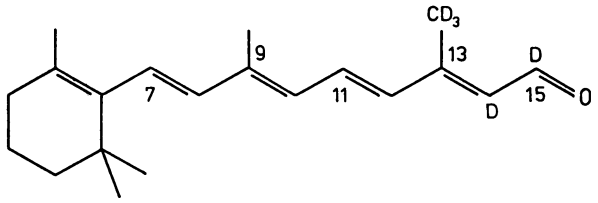

FIG. 1. Chemical structure of the synthetic [$^2H_5$]retinal as determined by ^1H NMR and mass spectroscopy. The chromophore structure is drawn in the 6-s-trans conformation (where "s" indicates "single bond") as observed in the ground state of bacteriorhodopsin (13). D, deuteron.

MATERIALS AND METHODS

Synthesis and Characterization of [$^2H_5$]Retinal. [$^2H_5$]Retinal (Fig. 1) was synthesized according to standard methods (14). The product was purified by chromatography and characterized by UV, ^1H NMR, and mass spectroscopy. The UV spectrum in ethanol was the same as that of undeuterated retinal. The mass spectrum had its maximum at m/z 289. The chemical shifts of the 270-MHz ^1H NMR spectrum had the expected values (15). From the lack of a proton signal at 2.33, 5.97, and 10.11 ppm and the mass peak at 289, we conclude that the end product of the synthesis corresponds to the structure shown in Fig. 1, with one deuteron each at C-14 and C-15 and three deuterons in the C-13 methyl group. The overall level of enrichment was 90%.

Regeneration of the Retinal-Minus Mutant JW5. Undeuterated retinal or [$^2H_5$]retinal was added to the growth medium of the retinal-minus mutant JW5 on the third, fourth, and

The publication costs of this article were defrayed in part by page charge payment. This article must therefore be hereby marked "*advertisement*" in accordance with 18 U.S.C. §1734 solely to indicate this fact.

*Present address: Weltraum Institut Berlin GmbH, Lassenstrasse 11-15, D-1000 Berlin 33, F.R.G.

fifth day of growth as described (11, 12). The purple membranes so regenerated had ratios of the absorbance at 280 and 568 nm of 1.47 (undeuterated retinal) and 1.51 ([$^2H_5$]-retinal) and were in all respects identical to native purple membranes.

Neutron Diffraction Experiments. The experiments were carried out as described in detail elsewhere (11, 12, 16). The deuterated and undeuterated samples contained 148 and 149 mg of bacteriorhodopsin, respectively. During the experiments the samples were enclosed at room temperature and 100% relative humidity in an aluminum can. The mosaic spread of both samples had a full width at half height of 12°. Both samples were in the beam for the same number of monitor counts (approximately 72 hr). The data were collected on the D-16 diffractometer of the Institut Laue–Langevin (Grenoble, France) at a wavelength of 4.52 Å.

RESULTS

Fig. 2 *a* and *b* show the raw neutron diffraction intensity data for samples of dark-adapted bacteriorhodopsin regenerated with undeuterated retinal and [$^2H_5$]retinal, respectively. The difference in neutron scattering length between [$^2H_5$]retinal and undeuterated retinal corresponds to about 10% of the scattering length of an average α-helix of bacteriorhodopsin (ref. 17, 10.4%; ref. 16, 9.2%). Clear intensity differences are thus expected. For instance, the intensity of the (*3,1*) reflection is about 15.5% larger for the undeuterated sample (Fig. 2*a*), whereas the intensity of the (*1,1*) reflection is larger for the deuterated sample (Fig. 2*b*) The largest intensity change was 15.5% and the average change was 4.4%. The intensity data are given in the second and third columns of Table 1. As a test for systematic errors and for reproducibility, the data were collected in the sequence [$^2H_5$]retinal-bacteriorhodopsin (24 hr), undeuterated retinal-bacteriorhodopsin (24 hr), [$^2H_5$]retinal-bacteriorhodopsin (48 hr), undeuterated retinal-bacteriorhodopsin (48 hr). The intensity differences for the 24-hr runs were the same as for the 48-hr runs. Distinct intensity differences were also observed in the lamellar diffraction pattern, confirming the incorporation of label. We have also collected data from a purple membrane sample regenerated with a partially deuterated retinal in which only the C-13 methyl group was deuterated. Apart from one reflection the signs of the intensity changes were the same as with the [$^2H_5$]retinal. Since the results with this [$^2H_3$]retinal were obtained with an entirely different sample during another machine run, this experiment shows convincingly that the observed intensity differences are reproducible and due to the partially deuterated retinals.

Table 1. Structure-factor differences

(*h,k*)	I_D	I_H	ΔF_{exp}	ΔF_{ref}	ΔF_{mod}	Phase, degrees
(*1,0*)	170.0	165.0	0.10	0.17	0.20	342
(*1,1*)	695.0	650.0	1.20	0.50	0.50	162
(*2,0*)	267.5	255.0	0.50	0.40	0.40	190
(*2,1*)	103.0	111.0	−0.30	−0.38	−0.30	210
(*1,2*)			−0.50	−0.44	−0.50	312
(*3,0*)	9.0	9.5	−0.10	−0.04	−0.10	96
(*2,2*)	37.0	37.0	0.00	−0.30	−0.20	118
(*3,1*)	60.0	71.0	−1.20	−0.82	−0.80	188
(*1,3*)			−0.30	−0.33	−0.30	120
(*4,0*)	32.0	32.0	0.00	−0.05	−0.10	282
(*3,2*)	32.5	30.5	0.40	−0.01	0.20	5
(*2,3*)			0.20	−0.19	−0.20	342
(*4,1*)	65.0	65.0	0.00	0.10	0.20	318
(*1,4*)			0.00	0.15	0.20	308
(*5,0*)	42.0	43.5	−0.30	−0.20	−0.20	345
(*4,2*)	64.0	63.0	0.10	0.54	0.50	103
(*2,4*)			0.20	−0.25	−0.10	240
(*5,1*)	25.5	27.0	0.00	−0.36	−0.50	28
(*1,5*)			−0.30	−0.12	−0.10	268
(*4,3*)	135.0	135.0	0.00	0.20	0.50	125
(*3,4*)			0.00	−0.12	−0.10	162
(*5,2*)	38.0	40.0	−0.40	−0.36	−0.20	130
(*2,5*)			−0.10	0.04	0.10	272

I_D and I_H are the experimental intensities for the [$^2H_5$]retinal and undeuterated retinal samples, respectively. $\Delta F = |F_D| - |F_H|$. ΔF_{exp} is the experimental structure-factor difference. ΔF_{ref} and ΔF_{mod} are the calculated structure-factor differences from the refinement and model calculations, respectively.

The data were analyzed as described (11, 12, 16). As a result of the almost identical sample preparation, the *sum* of the intensities of the deuterated sample was only 0.6% larger than the corresponding sum for the undeuterated sample. Under these circumstances, with a weak label and clear

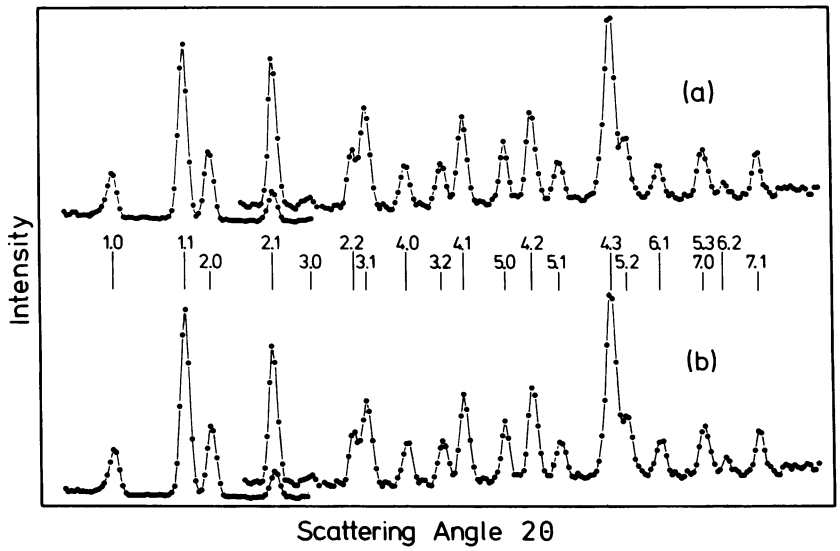

FIG. 2. Neutron diffraction patterns from oriented samples of dark-adapted purple membranes regenerated with retinal (*a*) and with [$^2H_5$]retinal (*b*) collected on the D-16 diffractometer of the Institut Laue–Langevin (Grenoble, France). Each reflection is labeled with the appropriate (*h,k*) index for a hexagonal lattice of unit-cell dimension 63 Å. Beginning with the (*2,1*) reflection, the vertical scale has been expanded by a factor of 5. From left to right the scattering angles of the data points vary from 2.25° to 40.05°. Both samples were in the beam for the same number of monitor counts (approximately 72 hr).

intensity differences, no further scaling is required. The experimental structure-factor differences (ΔF_{exp}) between the deuterated (F_D) and undeuterated (F_H) samples are collected in the fourth column of Table 1 [after correction of the intensities by a Lorentz factor of $(h^2 + hk + k^2)^{1/2}$]. Although well-resolved reflections were observed out to (*7,1*), beyond the (*5,2*) reflection no intensity differences occurred. The resolution corresponding to (*7,1*) is 7.2 Å. Fig. 3*a* shows the Fourier difference density map for the position of the deuterium label. Only one major difference peak occurs, which is twice as large as the next highest peak. The approximations used in the data analysis have been discussed in detail (11, 12, 16, 18). As in our previous work the phases (Table 1, last column) and the intensity ratios of nonequivalent reflections, which overlap in the powder pattern, were taken from the electron diffraction work (4, 5). In elaborate computer simulations these approximations were tested for the case of neutron diffraction with bacteriorhodopsin labeled with a [$^2H_{10}$]retinal (18). It was concluded that the label position can be retrieved with an accuracy of ±1 Å from data of moderate resolution such as used here [up to (*5,2*)] in spite of these approximations, provided the label is sufficiently weak. This is certainly the case with [$^2H_5$]retinal. The projected density of the purple membrane based on the neutron diffraction intensities of Fig. 2*a* in combination with the electron microscopy phases is shown in Fig. 4*a*.

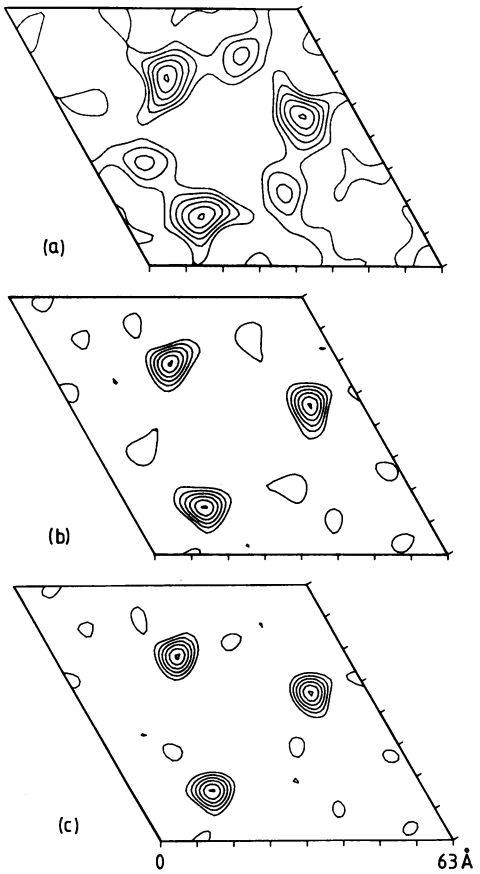

FIG. 3. (*a*) Two-dimensional Fourier difference map for the in-plane position of the center of deuteration of [$^2H_5$]retinal. There are three bacteriorhodopsin molecules per unit cell. The contour lines range from 0% (not shown) to 100% of the positive difference density in steps of 16.7%. There is one major peak per bacteriorhodopsin that is about twice as high as the second largest peak. (*b*) Fourier difference map for [$^2H_5$]retinal after refinement in reciprocal space (ΔF_{ref}). (*c*) Fourier difference map based on the model calculation (ΔF_{mod}).

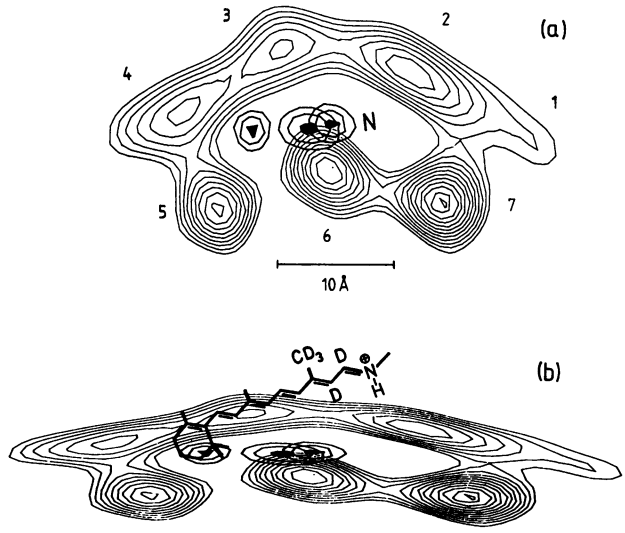

FIG. 4. The structure of the chromophore of bacteriorhodopsin as derived from neutron diffraction studies with three selectively deuterated retinals. (*a*) The 90%, 95%, and 99% contour lines for the three positive difference densities of (from left to right) the center of deuteration of the cyclohexene ring (12), the middle of the polyene chain (C-11) (11), and the center of deuteration of the Schiff base end of the polyene chain ([$^2H_5$]retinal) are shown in the interior of the protein. The three peaks are shown superimposed on the structure of bacteriorhodopsin as determined from the neutron intensities of Fig. 2*a*. The calculated position of the Schiff base nitrogen is indicated by the N. The seven helices are numbered according to the standard convention (8). (*b*) View in perspective with the plane of the membrane and the plane of the chromophore at right angles (19, 20). Above the projected two-dimensional structure of bacteriorhodopsin, the structure of all-trans retinal is drawn to scale in a plane perpendicular to the membrane with the polyene chain making a tilt angle of 20° (10). The chromophore is positioned so that the projections of the three labeled regions in the ring, the middle of the chain (C-11), and the Schiff base end of the chain fit well with the corresponding peaks in the difference density. In the structural formula of retinal the deuterium distribution is only shown for the $^2H_5$ label.

The position of the label site was refined by using a standard crystallographic program for the refinement of heavy-atom sites (21). In this procedure a point label is moved around in the neighborhood of the main peak until the "lack of closure" summed over all reflections is minimal (12, 16, 21). This procedure gets around some of the limitations of the Fourier difference approach (16). Using the "refined" F_D values, new Fourier difference coefficients ΔF_{ref} were calculated (Table 1) and the corresponding Fourier difference map is presented in Fig. 3*b*. The refinement did not change the position of the major peak but substantially reduced the amplitudes of the secondary maxima in Fig. 3*a*. After refinement the major difference peak is 4–5 times larger than the next highest peak. A comparison of columns 4 and 5 of Table 1 shows that the refinement changed the signs of only a few reflections with small Fourier difference coefficients. Model calculations were also carried out to find out whether the difference map had the amplitude expected for a retinal labeled with five deuterons (as described in refs. 12 and 16). The extra density corresponding to the label was added at the point determined in the refinement procedure. The predicted Fourier difference coefficients ΔF_{mod} (Table 1) are in excellent agreement with the coefficients from the refinement calculation, and the corresponding Fourier difference plot (Fig. 3*c*) is accordingly very similar to that of Fig. 3*b*. The results of the model calculation show that the Fourier difference map of Fig. 3*a* has the appropriate amplitude expected for the label. We note from Table 1 that the

model calculation predicts the sign of all the major reflections correctly. The predicted amplitudes differ considerably from the measured ones. It is well known, however, that the phases determine the quality of the Fourier difference map and that as long as the signs of the major Fourier difference coefficients are right, the correct position is obtained even with unit amplitudes for all reflections (22). Since we have used retinals with 10 and 11 deuterons in our previous work (11, 12), we also have an internal calibration standard to check whether the difference map has the correct amplitude. After the intensities are normalized, the peak amplitudes of the Fourier difference maps for the [$^2H_{10}$]-, [$^2H_{11}$]-, and [$^2H_5$]retinal should have the ratios 10:11:5, in good agreement with the actual ratios of 12:9:5.

DISCUSSION

The present work on the position of the Schiff base end of the chromophore is presented together with our previous results on the cyclohexene ring (12) and the middle of the chain (11) in Fig. 4*a*. All three Fourier difference peaks lie approximately on one line. This is to be expected if the plane of the chromophore is perpendicular to the plane of the membrane, as was recently suggested by polarized infrared (19) and resonance Raman (20) spectroscopy. Note that the difference density for the middle of the chain is elongated in the direction of the line connecting the three peaks [this can be observed more clearly in the original Fourier difference map (11)]. This is consistent with the proposed collinear geometry, since for this labeled retinal the deuteration is concentrated in the two methyl groups at C-9 and C-13, which are symmetrically arranged along the line with respect to C-11. The predicted distances between the three Fourier difference peaks, assuming the C-6–C-7 bond to be trans (13) and the tilt angle of the polyene chain to be 20° (10), are about 5.0 Å for the distance between the deuterated cyclohexene ring and the middle of the polyene chain (C-11) and about 2.4 Å for the distance between C-11 and the $^2H_5$-label near the Schiff base. According to Fig. 4*a* these distances are 4.9 Å and 2.0 Å. Considering the errors in both this calculation and the diffraction experiment, the agreement is good indeed. The calculation did not take into account the fact that the sample was dark-adapted, containing 13-*cis*- and all-*trans*-retinal in a 1:1 ratio. Experimentally we observe only one peak for the Schiff base label that is not elongated. Only the position of the deuterium at C-15 will differ in the 13-cis form from that in the all-trans form if we assume again that the planes of the chromophore and the membrane are perpendicular. The distance between the $^2H_5$-label and the center of the chain is thus only slightly less in the dark-adapted state. This explains why only one peak is observed and may explain why the observed distance of 2.0 Å is somewhat smaller than expected.

The in-plane position of the Schiff base nitrogen may now be estimated by extrapolation along the line. Its exact position depends only slightly on whether the polyene chain tilts up (as shown in Fig. 4*b*) or down with respect to the membrane plane. Assuming the cis–trans isomerization to take place in the plane perpendicular to the membrane, we obtain the position marked N in Fig. 4*a*. It corresponds to the projection of the Schiff base nitrogen onto the plane of the membrane with the chromophore in the all-trans state, as shown in Fig. 4*b*. Drawing a circle of 8 Å around this point, corresponding to the distance from the amino nitrogen of a perpendicularly extended lysine side chain to the center of an α-helix, one finds that only the centers of helices 2 and 6 fall within the circle. Helix G is thus either 2 or 6. The result of Fig. 4*a* establishes the orientation of the polyene chain of the chromophore within the projected structure and shows with which helices the chromophore and, in particular, the Schiff base may interact in the course of proton translocation.

Previous work with perdeuterated retinal (28 deuterons) led to contradictory results concerning the center of mass of the whole chromophore (17, 23). This discrepancy is now resolved: the initial report (23) must have been in error. It is interesting that fluorescence energy-transfer experiments have been quite useful in obtaining a low-resolution position of the chromophore. From a determination of the distance of closest approach between a fluorescent donor in the lipid phase and the acceptor retinal, it was concluded that the chromophore was at the center of the protein with an excluded volume radius of 18 Å, in reasonable agreement with the present results (24). Using an entirely different fluorescence approach (25), six equally likely chromophore positions were found, one of which was in fair agreement with the present result. No reason for this particular choice was offered, however, and the orientation of the polyene chain was only in weak agreement with our result.

Apart from the availability of a sufficient amount of machine time on a well-designed diffractometer, we believe that the sample preparation is the key to successful neutron diffraction work with weakly labeled membrane systems. In order to minimize the generation of differences that were not due to the labeling, extreme care was taken in all phases of the preparation to handle the deuterated and undeuterated sample in the same way. Manipulations such as the growth of cells, cell harvesting, formation of oriented purple membrane films, and centrifugations were performed in parallel with the same media and solvents.

We have shown that, by careful sample preparation, the sensitivity of neutron diffraction measurements may be increased to the point that small functional groups containing only five deuterons can be located within a membrane protein. This opens up applications to many other systems. With the label at a functionally significant site, it may be possible to observe conformational changes in the course of an enzyme's action. With the present system it will be interesting to see if the trans–cis isomerization of the chromophore that occurs during the photocycle may be observed directly.

This research was carried out at the Institut Laue–Langevin (Grenoble) and has benefitted from the excellent instrumentation available in this laboratory. We thank J. Torbet for his help as local contact on the D-16 diffractometer and R. Henderson for providing us with the phases and structure-factor ratios from the electron diffraction work. We acknowledge the advice of J. Lugtenburg on the synthesis of [$^2H_5$]retinal. This work was supported by grants (to M.P.H.) from the Bundesministerium für Forschung und Technologie (03 BU1 FUB-6) and from the Deutsche Forschungsgemeinschaft (Sfb 312).

1. Stoeckenius, W. & Bogomolni, R. A. (1982) *Annu. Rev. Biochem.* **52,** 587–616.
2. Henderson, R. (1975) *J. Mol. Biol.* **93,** 123–138.
3. Blaurock, A. E. (1975) *J. Mol. Biol.* **93,** 139–158.
4. Unwin, P. N. T. & Henderson, R. (1975) *J. Mol. Biol.* **94,** 425–440.
5. Henderson, R. & Unwin, P. N. T. (1975) *Nature (London)* **257,** 28–32.
6. Hayward, S. B. & Stroud, R. M. (1981) *J. Mol. Biol.* **151,** 491–517.
7. Agard, D. A. & Stroud, R. M. (1982) *Biophys. J.* **37,** 589–602.
8. Engelman, D. M., Henderson, R., McLachlan, A. D. & Wallace, B. A. (1980) *Proc. Natl. Acad. Sci. USA* **77,** 2023–2027.
9. Henderson, R., Baldwin, J. M., Downing, K. H., Lepault, J. & Zemlin, F. (1986) *Ultramicroscopy* **19,** 147–178.
10. Heyn, M. P., Cherry, R. J. & Müller, U. (1977) *J. Mol. Biol.* **117,** 607–620.
11. Seiff, F., Wallat, I., Ermann, P. & Heyn, M. P. (1985) *Proc. Natl. Acad. Sci. USA* **82,** 3227–3231.

12. Seiff, F., Westerhausen, J., Wallat, I. & Heyn, M. P. (1986) *Proc. Natl. Acad. Sci. USA* **83,** 7746–7750.
13. Harbison, G. S., Smith, S. O., Pardoen, J. A., Courtin, J. M. L., Lugtenburg, J., Herzfeld, J., Mathies, R. A. & Griffin, R. G. (1985) *Biochemistry* **24,** 6955–6962.
14. Lugtenburg, J. (1985) *Pure Appl. Chem.* **57,** 753–762.
15. Patel, D. (1969) *Nature (London)* **221,** 825–827.
16. Seiff, F., Wallat, I., Westerhausen, J. & Heyn, M. P. (1986) *Biophys. J.* **50,** 629–635.
17. Jubb, J. S., Worcester, D. L., Crespi, H. L. & Zaccai, G. (1984) *EMBO J.* **3,** 1455–1461.
18. Plöhn, H.-J. & Büldt, G. (1986) *J. Appl. Crystallogr.* **19,** 255–261.
19. Earnest, T. N., Roepe, P., Braiman, M. S., Gillespie, J. & Rothschild, K. J. (1986) *Biochemistry* **25,** 7793–7798.
20. Ikegami, A., Kouyama, T., Kinosita, K., Otomo, J., Urabe, H., Fukuda, K. & Kataoka, R. (1987) in *Retinal Proteins*, ed. Ovchinnikov, Y. (VNU Science Press, Utrecht, The Netherlands), pp. 37–45.
21. Dickerson, R. E., Weinzierl, J. E. & Palmer, R. A. (1968) *Acta Crystallogr. B* **24,** 997–1003.
22. Blundell, T. L. & Johnson, L. N. (1976) *Protein Crystallography* (Academic, New York).
23. King, G. I., Mowery, P. C., Stoeckenius, W., Crespi, H. L. & Schoenborn, B. P. (1980) *Proc. Natl. Acad. Sci. USA* **77,** 4726–4730.
24. Rehorek, M., Dencher, N. A. & Heyn, M. P. (1983) *Biophys. J.* **43,** 39–45.
25. Kouyama, T., Kimura, Y., Kinosita, K. & Ikegami, A. (1982) *J. Mol. Biol.* **153,** 337–359.